PERSONALIZED MEDICINE RECOMMENDATION SYSTEM FOR VARIOUS LUNG CANCER TYPES USING FDHSCNN AND LIME-FWPIMS

Sanjuktarani Jena[1], Upendra Kumar [2,3], Sai Kiran Oruganti [4]

[1] Department of Computer Engineering, Sardar Patel Institute of Technology, Mumbai, India.

[2] Department of Computer Science Engineering, Institute of Engineering and Technology, Lucknow, India.

[3] Lincoln University College, Malaysia.;

[4] Lincoln University College, Malaysia.

sanjuktarani.jena@spit.ac.in; upendra.ietlko@gmail.com; saisharma@lincoln.edu.my;

Abstract: Personalized medicine plays a vital role in improving accuracy in diagnosis and treatment planning for lung cancer by patient-specific imaging and computational intelligence. This paper proposes a Personalized Medicine Recommendation System for Various Lung Cancer Types based on a Feature-Driven Hierarchical Spatial Convolutional Neural Network (FDHSCNN) combined with an explainable framework named Local Interpretable Model-agnostic Explanations (LIME)based Feature-Weighted Personalized Inference and Mapping System (LIME-FWPIMS). The proposed system utilizes multimodal PET–CT images to capture both functional and anatomical tumor characteristics, allowing for precise classification of multiple lung cancer subtypes.

The FDHSCNN architecture hierarchically learns discriminative spatial and deep semantic features, improving robustness and classification performance while mitigating overfitting. To enhance transparency and reliable clinical outputs, LIME-FWPIMS is employed to generate localized, feature-weighted explanations, supporting interpretable and personalized clinical decision-making. Experimental evaluation on PET–CT datasets demonstrates that the proposed method achieves a high classification accuracy of a 99.07%, outperforming existing deep learning–based approaches.

The results indicate that integrating advanced deep feature learning with explainable artificial intelligence, significantly enhances diagnostic reliability and personalized treatment recommendation. The proposed framework shows strong potential for deployment in precision oncology applications, offering accurate, interpretable, and patient-centric lung cancer diagnosis.

Keywords: *Computed Tomography (CT) images, Positron Emission Tomography/Computed Tomography (PET/CT), Lung Tumor Segmentation, Deep Learning (DL), and Local Density Harmonization*

1. INTRODUCTION

Lung cancer (LC) has emerged as one of the leading causes of cancer-related deaths worldwide, and accounts for a staggering one-sixth of global deaths [1]. It is a result of rapid, uncontrolled proliferation of malignant cells within lung tissues, which leads to formation of a tumor mass and aggressive disease progression [2], [3]. It has a pleomorphic tendency and high fatality rate, thus making accurate classification and stage-specific diagnosis of LC critical for effective treatment planning [4].

Medical imaging modalities such as Magnetic Resonance Imaging (MRI), Positron Emission Tomography (PET), and Computed Tomography (CT) play a central role in LC diagnosis [5]. PET provides important metabolic information; however, it is unable to provide detailed anatomical context when used independently [6], [7]. The integration of PET and CT into a unified PET/CT imaging framework addresses this limitation by offering characteristic metabolic and anatomical insights, which will improve lesion characterization and disease staging [8], [9].

Recent advances in Machine Learning (ML) and Deep Learning (DL) have enhanced computer-aided diagnosis by enabling automated feature extraction and high accuracy of diagnosis [10], [11]. However, existing approaches are often held back as they get limited in terms of generalization and fail to deliver personalized, stage-aware treatment recommendations for all the diverse LC types [12], [13]. Motivated by these limitations, this paper proposes a PET/CT-based, LC stage-aware personalized medicine recommendation framework using FDHSCNN integrated with LIME-FWPIMS, aiming to improve diagnostic accuracy, interpretability, and individualized clinical decision support.

1.1 Problem Statement

The limitations are depicted as follows:

1. None of the conventional works aimed at providing personalized medicine recommendations across all LC stages based on varying factors like tumor histology and patient characteristics, including age, overall health, and comorbidities.
1. Due to multiple variations such as lung tissue density and anatomical structures seen in patients, some traditional works struggled to detect and characterize tumors accurately.
2. Owing to the overlapping anatomical structures, low contrast boundaries, and variable tumour shapes, [14] struggled to segment lung nodules and tumours in CT images.
3. Some previous works relied on black-box AI models and failed to form a clear explaination, leading to reduced clinical tract and decision-making accuracy.

1.2 Objectives

The proposed framework's major objectives are demonstrated as follows:

1. The proposed LIME-FWPIMS framework is employed to deliver personalized treatment recommendations tailored to different stages of lung cancer (LC).
2. To enable the identification of early-stage LC with subtle and low-contrast abnormalities, a Contrast-Limited Gaussian-Weighted Tile Blending Histogram Equalization (CLGWTBHE)–based image contrast enhancement approach integrated with image pyramid construction is introduced.
2. 3.The proposed Cumulative Tissue Density Distribution Interpolation Statistics (CTDDIS) and Fuzzy C-Means (FCM) techniques are utilized to analyze lung tissue density variations and anatomical structural differences across patients, respectively.
3. For accurate segmentation of lung nodules and tumors and effective differentiation of overlapping boundaries, the proposed Adaptive Anisotropic Smoothing Graph Cut (AASGC) and Selective Skip Injection Segmentation Network (SSI-SegNet) are employed, respectively.

4. The proposed Feature-Driven Hierarchical Spatial Convolutional Neural Network (FDHSCNN) is applied to classify multiple lung cancer types and stages by jointly leveraging lifestyle-related clinical attributes and imaging features.
5. 6.To enhance model transparency and clinical interpretability within the personalized medicine recommendation system, Local Interpretable Model-Agnostic Explanations (LIME) are incorporated.

2. RELATED WORK

[14] designated a model for LC detection and staging. Here, CT images were collected and pre-processed, followed by lesion identification. Next, to extract the features for subtype classification, the You Only Look Once version-8 (YOLOv8) was applied. Lastly, the Tumor, Node, and Metastasis Classifier (TNMClassifier) classified the various stages with 98% accuracy. However, this model failed to differentiate overlapping anatomical structures, leading to inaccurate tumor segmentation.

[15] presented a framework for LC detection and classification by employing PET/CT images. Here, the Residual Network-50 (ResNet-50) extracted the feature representations. Also, to classify the lung lesions into T-stages and histological types, the transformer was utilized, attaining 0.97 accuracy. This model had inefficient performance in the LC stage classification owing to the reliance on imaging data and overlooking demographic information.

[16] offered a dual-output classification model for histological types and stage classification using radiomic features extracted as of lung CT images. Here, radiomic features were extracted. Next, Pearson correlation and Lasso regression were applied to select optimal features. Lastly, LC subtypes and stages were classified with 98% accuracy. Nevertheless, this model had a small sample size, affecting the training efficiency and generalization capability.

[17] presented a multi-stage intermediate fusion pipeline to classify non-small cell LC subtypes using PET and CT images. Also, the features from both PET and CT images were fused. Lastly, the multimodal 3D ResNet classified the subtypes with 0.762 accuracy. But, due to its limited ability to capture fine spatial information, the system did not perform well across diverse LC types.

[18] offered an interpretable LC diagnostic model by integrating multiple CT datasets. Here, five heterogeneous CT datasets were used, followed by feature extraction. Afterward, the Mobile Network Version-3 (MobileNetV3) performed the LC classification with ~99% accuracy. Lastly, by using Gradient-weighted Class Activation Mapping (Grad-CAM), the interpretability was enhanced. Nevertheless, due to its lightweight nature, the model struggled to capture intricate patterns.

[19] applied the Retina U-Net model for automated detection and staging of LC lesions. Here, this model performed data augmentation and oversampling. Lastly, to classify lesions as TNM, the Retina U-Net was applied, attaining ~90% accuracy. This model introduced inter-observer variability as lesion segmentation was conducted manually.

[20] presented a one-stage CT-based lung tumour detection model optimized for multi-scale performance. Here, to extract spatial features of PET/CT images, the YOLOv7 was applied. Also, to capture diverse contextual information, the Receptive Field Enhancement Modules (RFEMs) were incorporated for accurate lung tumor detection. As per the result, this model attained 0.967 precision. Nevertheless, due to the increased number of parameters, this model had a computational complexity issue.

[21] established the Deep Ensembled Multimodal Fusion (DEMF) model for LC classification using CT and PET images. Here, the DEMF classified the LC using the pre-trained Convolutional Neural Networks (CNNs) with 0.976 accuracy. Lastly, Grad-CAM visualization enhanced the model's interpretability. Nevertheless, this model failed to capture non-linear relationships across lung regions.

3. PROPOSED METHODOLOGY

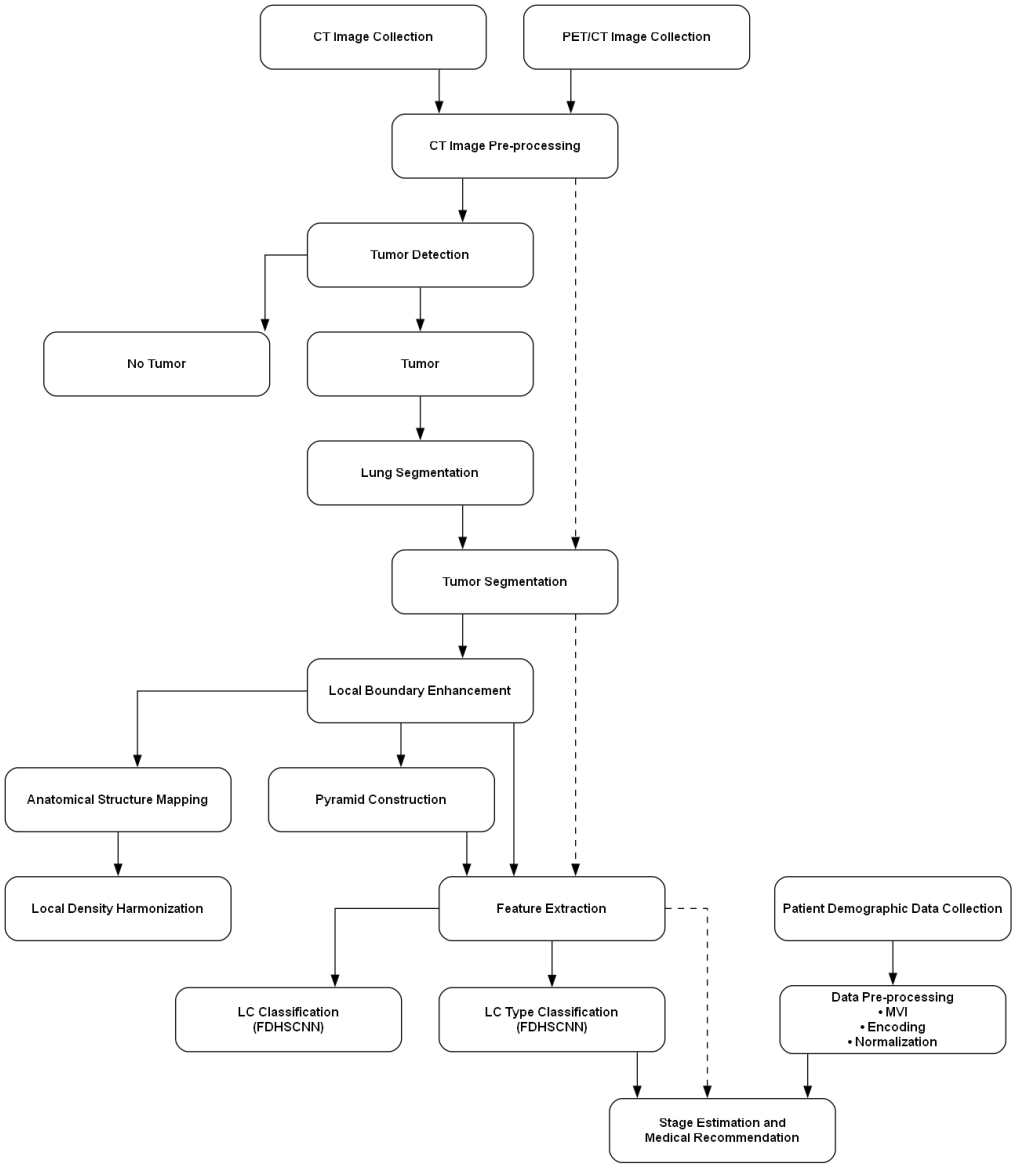

Figure 1: Block Diagram for the proposed framework

3.1 Overview of the Proposed Framework

In this work, CT images, PET/CT fused images, and patient demographic data are jointly analysed to propose an integrated intelligent framework for early-stage lung cancer (LC) detection, segmentation, classification, stage estimation, and personalised medical recommendation. CT image preprocessing, tumor detection, lung and tumor segmentation, local density harmonisation, anatomical structure mapping, boundary enhancement, multi-scale feature extraction, LC classification, malignancy type classification, demographic preprocessing, stage estimation, and treatment recommendation comprise the sequential modules of the framework, as shown in the block diagram.

3.2 CT Image Collection and Preprocessing

Lung CT scans from publicly available sources are utilized to train models for the classification of LC and the evaluation of tumours. A robust preprocessing scheme is utilized as CT scans often exhibit noise, low contrast, and minute pathologies, which are common, especially when LC is in the early stages. A uniformity scheme is introduced to ensure all CT scans are reduced to a standard resolution to facilitate training. CLGWTBHE is employed to emphasis faint nodules. Compared to standard CLAHE, the proposed Gaussian-weighted tile blending reduces block artefacts and smoothes intensity transitions between nearby tiles. Finally, high-quality preprocessed CT images are created using Bilateral Filtering (BF) to minimise noise while preserving critical edge information.

3.3 Tumor Detection Using FDHSCNN

The tumors are detected with the proposed Feature-Dependent Hyperparameter Scheduling Convolutional Neural Network. Although conventional CNNs capture the spatial characteristics better, due to their predefined hyperparameters, they converge slowly.
In this way, FDHSCNN dynamically updates learning rate, batch size, and optimiser parameters based on the quality of features; hence, it converges faster and is more stable. The network consists of a fully connected layer with sigmoid activation, pooling layers for spatial reduction, and convolutional layers with ReLU activation. By this approach, CT scans from tumors and non-tumors are correctly classified.

3.4 Lung and Tumor Segmentation Using SSI-SegNet

For tumor-detected cases, precise lung area and tumor segmentation is essential. Consequently, the Selective Skip Injection Segmentation Network, or SSI-SegNet, is employed.
The encoder derives hierarchical feature representation through convolutional and max-pooling layers, whereas in the decoder, spatial detail is reconstructed through up sampling. Unlike in conventional SegNet, in Selective Skip Injection (SSI), injection of features in the encoder is performed in high detail

regions to avoid over-smoothing. This allows for the accurate separation of lung regions and small tumors with clear borders.

3.5 Local Density Harmonization & Anatomical Structure Mapping

The variation in the lung tissue densities is removed from the segmented lung images by the use of the Cumulative Tissue Density Distribution Interpolation Statistics (CTDDIS). The region of the lung is divided into small areas, and the statistical values such as the mean and the standard deviation are calculated. A method known as the Cumulative Distribution Interpolation (CDI) is responsible for the creation of continuity among the neighboring areas in the lung region, thereby omitting the boundary effects. The use of fuzzy C-Means (FCM) clustering is responsible for the mapping of the anatomical parts, which is a sensitive process in the creation of the lung lobes, blood vessels, as well as the bronchi.

3.6 Local Boundary Enhancement and Tumor Segmentation

Since the borders of lung tissues, nodules, and tumors overlap, Adaptive Anisotropic Smoothing-based Graph Cut (AASGC) is presented for local boundary augmentation. Anisotropic smoothing treats small nodules and irregular tumor formations, by minimizing excessive smoothing around areas with high curvature. It models pixels as graph nodes with weighted edges. After the boundary augmentation, SSI-SegNet is used again to segment tumor patches and accurately localize small abnormalities.

3.7 Pyramid Construction and Feature Extraction

A picture pyramid that collects multi-scale contextual information is created by gradually down sampling segmented tumor photographs. Each pyramid level highlights tumor features at different spatial resolutions, making it easier to spot small and irregular formations. Tumor-segmented images and pyramid representations are used to recover a variety of shape, textural, statistical, and multi-scale features. These include fractal dimension, area, perimeter, eccentricity, solidity, texture contrast, energy, gradient magnitude, and frequency components.

3.8 Lung Cancer Classification and PET/CT Analysis

Using the collected features, FDHSCNN classifies LC cases as benign or malignant. Relevant PET/CT fused images are collected for malignant cases to facilitate accurate malignancy type classification. The images from the PET/CT scan, similar to CT scans, also go through image processing, segmentation, and feature extraction. Based on morphology and metabolism, FDHSCNN diagnoses LC into adenocarcinoma, small-cell carcinoma, large-cell carcinoma, and squamous-cell carcinoma.

3.9 Demographic Data Processing, Stage Estimation, and Medical Recommendation

The patient demographic features, such as age, gender, smoking history, family history, and comorbidities, are gathered and pre-processed using the mean imputation technique, category encoding, and Z-score normalization. Finally, the LIME FW PMIS approach is used for the estimation of the stage of LC and the development of patient-specific treatment plans. The Gaussian fuzzy membership techniques transform the patient clinical and imaging features into fuzzy sets, while the Weighted Pattern Mining technique defines the priority level. The therapeutic trust is improved using the interpretation delivered by the feature contribution to predict the outputs of the LIME approach.

The fuzzy rule is generated to estimate LC stages and their corresponding treatment recommendation with respect to the Weighted Pattern Mining (WPM). Here, the LC stages estimation rule (R^{Sta}) is created based on the tumor size (tis, t1mi, t1a, t1b, t1c, t2a, t2b, t3, t4), nodal involvement (n0, n1, n2, n3, n4), and metastasis (m0, m1a, m1b, m1c). Based on the LC stages (0, IA1, IA2, IA3, IB, IIA, IIB, IIIA, IIIB, IIIC, IVA, IVB, and IV), the medicine recommendation rule is developed.

$$\mathfrak{R}^{Sta} = \begin{cases} \text{If } (t_{is}, n_0, m_0) & ; 0 \\ \text{If } [(t_{1mi}, n_0, m_0), (t_{1a}, n_0, m_0)] & ; IA1 \\ \text{If } (t_{1b}, n_0, m_0) & ; IA2 \\ \text{If } (t_{1c}, n_0, m_0) & ; IA3 \\ \text{If } (t_{2a}, n_0, m_0) & ; IB \\ \text{If } (t_{2b}, n_0, m_0) & ; IIA \\ \text{If } [(t_{1a}, n_1, m_0), \ldots, (t_{2a}, n_1, m_0), \ldots, (t_3, n_0, m_0)] & ; IIB \\ \text{If } [(t_{1a}, n_2, m_0), \ldots, (t_{2a}, n_2, m_0), \ldots, (t_3, n_1, m_0), (t_4, n_0, m_0), \ldots] & ; IIIA \\ \text{If } [(t_{1a}, n_3, m_0), \ldots, (t_{2a}, n_3, m_0), \ldots, (t_3, n_2, m_0), (t_4, n_2, m_0)] & ; IIIB \\ \text{If } [(t_3, n_3, m_0), (t_4, n_4, m_0)] & ; IIIC \\ \text{If } [(\text{any } t, \text{ any } n, m_{1a}), (\text{any } t, \text{any } n, m_{1b})] & ; IVA \\ \text{If } (\text{any } t, \text{ any } n, m_{1c}) & ; IVB \\ \text{If } (\text{any } t, \text{ any } n, m_1) & ; IV \end{cases}$$

$$\mathfrak{R}^{Rec} = \begin{cases} \text{If } (0) & ; \text{Surgical resection} \\ \text{If } (IA1) & ; \text{Surgical resection, SBRT} \\ \text{If } (IA2) & ; \text{Surgery} \pm AC \\ \text{If } (IA3) & ; \text{Surgery} \pm AC(\pm\text{immunotherapy}) \\ \text{If } (IB) & ; \text{Surgery} + AC(\pm\text{immunotherapy}) \\ \text{If } (IB \text{ or } IIA) & ; \text{Surgery} + AC \pm \text{immunotherapy} \\ \text{If } (IIB) & ; \text{Surgery} + AC \pm \text{immunotherapy, Radiation} \\ \text{If } (IIIA) & ; \text{Multimodal: Surgery + chemoradiation + immunotherapy} \\ \text{If } (IIIB) & ; \text{Con - chemoradiation + surgery, Consol - immunotherapy} \\ \text{If } (IIC) & ; \text{Def - chemoradiation} \pm \text{immunotherapy} \\ \text{If } (IVA) & ; \text{Sys - chemoradiation} \pm \text{immunotherapy, Pall - radiation} \\ \text{If } (IVB) & ; \text{Same as IVA, Sys - therapy \& Symptom Relief} \\ \text{If } (IV) & ; \text{Sys - therapy, Pall - care} \end{cases}$$

Where, (any t, any n) exemplifies (tis, t1mi, t1a, t1b, t1c, t2a, t2b, t3, t4) and (n0, n1, n2, n3, n4), respectively, and (SBRT, AC) indicates the Stereotactic Body Radiation Therapy and Adjuvant Chemotherapy, correspondingly.

4. RESULT AND DISCUSSION

Table 1: Dataset Details

Dataset	Training	Testing
IQ-PTH/NCCD	1035	259
Lung CT nodules/Lesion Segmentation	4055	1014
Lung-PET-CT-Dx	855	214

Table 2: Image Results for LC Type Classification

Steps	Adenocarcinoma	Small-cell Carcinoma	Large-cell carcinoma	Squamous-cell Carcinoma
PET/CT input	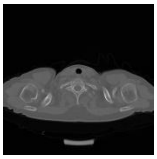	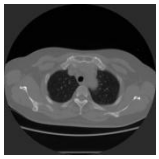	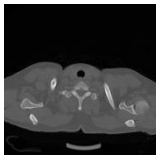	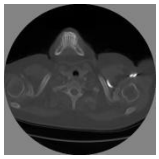
PET/CT resizing	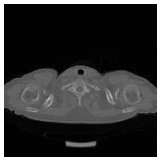	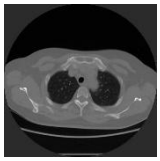	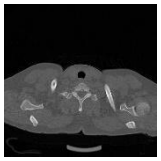	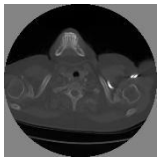
PET/CT contrast enhancement	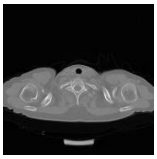	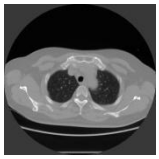	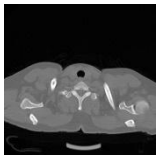	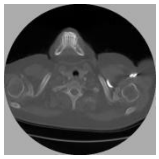
PET/CT noise removal	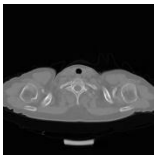	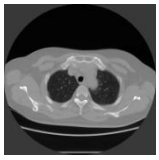	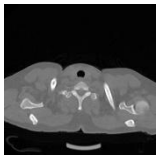	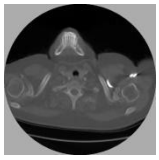
PET/CT tumor segmentation	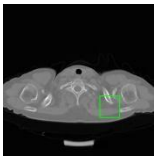	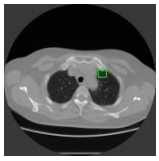	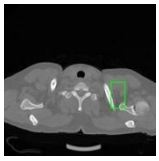	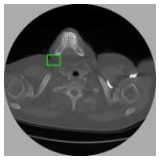

The sample image results for various LC types, like adenocarcinoma, large-cell carcinoma, small-cell carcinoma, along with squamous-cell carcinoma, by processing the patients' PET/CT fused images, are depicted in Table 2.

4.1 Performance Evaluation for the Proposed Work

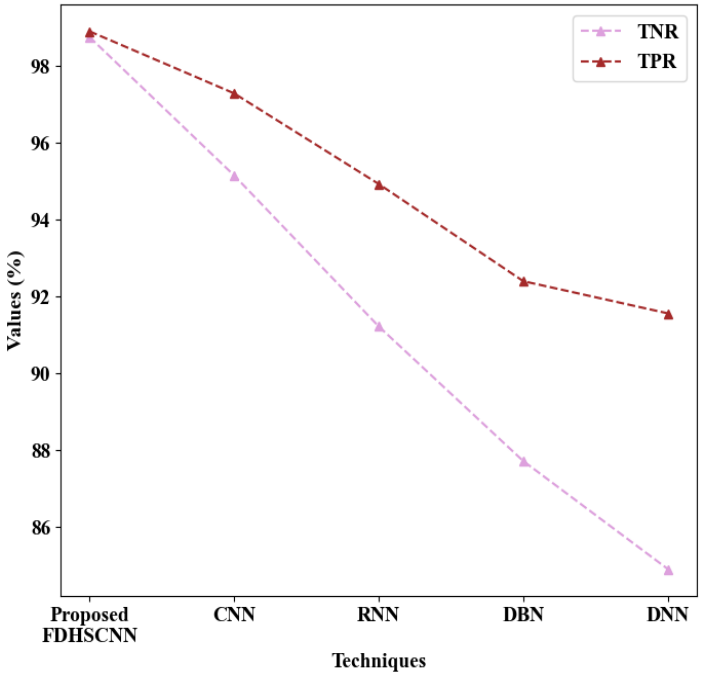

Figure 2: Efficiency Analysis for Tumor Detection

Table 3: Empirical Evolution for Tumor Detection

Metrics/Techniques	Proposed FDHSCNN	CNN	RNN	DBN	DNN
Accuracy (%)	99.07407	97.22222	94.44444	92.09302	89.81481
TPR (%)	99.08257	98.50746	95.4955	93.33333	92.96875
TNR (%)	99.06542	95.12195	93.33333	90.52632	85.22727

Table 4: Empirical Analysis for LC type classification

Metrics/Methods	Proposed FDHSCNN	CNN	RNN	DBN	DNN
Precision (%)	98.14815	95.45455	92.30769	90.7563	86.23853
Sensitivity (%)	99.06542	96.33028	94.73684	92.30769	88.67925
Recall (%)	99.06542	96.33028	94.73684	92.30769	88.67925

F-measure (%)	98.60465	95.89041	93.50649	91.52542	87.44186
Accuracy (%)	98.58491	95.75472	92.92453	90.56604	87.26415
Specificity (%)	98.09524	95.14563	90.81633	88.42105	85.84906

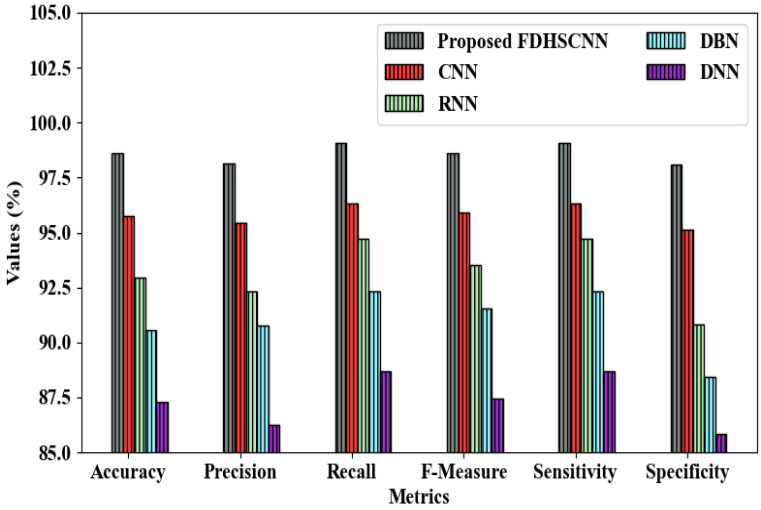

Figure 3: Efficacy Evaluation for LC type classification

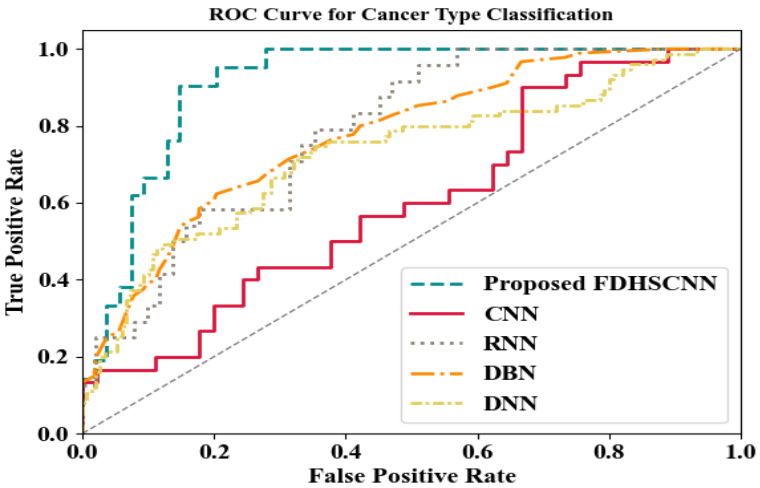

Figure 4: ROC analysis for LC type classification

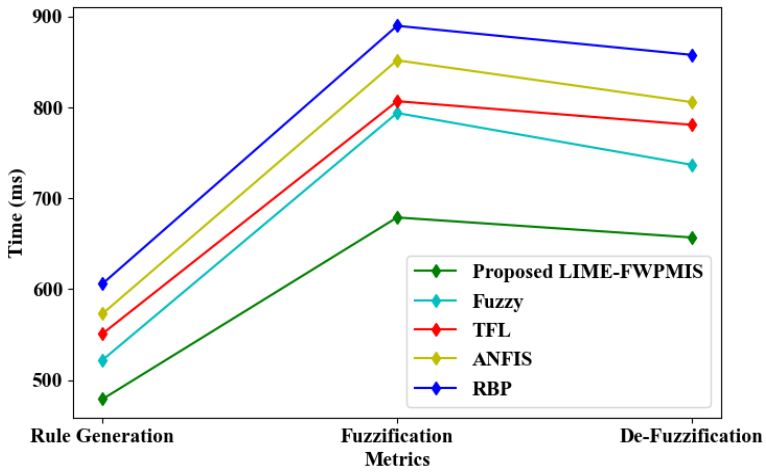

Figure 5: Time Analysis

Table 5: Numerical Validation for the proposed LIME-FWPMIS

Metrics/Techniques	Proposed LIME-FWPMIS	Fuzzy	TFL	ANFIS	RBP
Rule Generation Time (ms)	479	522	551	573	606
Fuzzification Time (ms)	679	794	807	852	890
Defuzzification Time (ms)	657	737	781	806	858

The proposed LIME-FWPMIS demonstrates superior efficiency by significantly reducing rule generation (479ms), fuzzification (679ms), and defuzzification (657ms) times for accurate stage estimation and relevant treatment recommendation

5. CONCLUSIONS

This study presented an effective PET/CT image–based, stage-aware personalized treatment recommendation framework using multiple lung cancer (LC) classification models. Initially, tumors were detected from CT lung images using the FDHSCNN, achieved an accuracy of 99.074%. Subsequently, the SSI-SegNet model effectively segmented the lung regions, while CTDDIS performed precise local density harmonization. In addition, boundaries of lung regions were significantly enhanced, achieving an edge preservation index (EPI) of 0.9313.

For early-stage LC classification, the SSI-SegNet efficiently stratified and sorted tumors from lung images, with the FDHSCNN attaining an accuracy of 98.8439%. PET/CT fused images were then used to accurately classify different LC types, resulting in a classification accuracy of 98.5849% based on extracted image features. Finally, cancer stages were accurately estimated, and appropriate treatment recommendations were generated using the LIME-FWPMIS approach by taking into factor tumor size, lymph node involvement, and metastasis.

Overall, the proposed framework outperformed conventional methods by offering a comprehensive, accurate, and efficient solution for lung cancer diagnosis and personalized treatment recommendation.

Future Scope

Future work will focus on incorporating information on molecular mutations and biomarkers, derived from genomic data to further improve lung cancer subtype classification and to support progression-based personalized treatment recommendations.

References

[1] Safarian, A., Mirshahvalad, S. A., Nasrollahi, H., Jung, T., Pirich, C., Arabi, H., & Beheshti, M. (2025). Impact of [18F] FDG PET/CT Radiomics and Artificial Intelligence in Clinical Decision Making in Lung Cancer: Its Current Role. *Seminars in Nuclear Medicine*, *55*(2), 156–166. https://doi.org/10.1053/j.semnuclmed.2025.02.006

[2] Nguyen, D. T., Nguyen, T. T., Nguyen, H. T., Nguyen, T. T., Pham, H. H., Nguyen, T. H., Truong, T. N., & Le Nguyen, P. (2024). CT to PET Translation: A Large-scale Dataset and Domain-Knowledge-Guided Diffusion Approach. *ArXiv*, 1–10. https://arxiv.org/pdf/2410.21932

[3] Ji, Y., Qiu, Q., Fu, J., Cui, K., Chen, X., Xing, L., & Sun, X. (2021). Stage-specific PET radiomic prediction model for the histological subtype classification of non-small-cell lung cancer. *Cancer Management and Research*, *13*, 307–317. https://doi.org/10.2147/CMAR.S287128

Qu, J., Han, X., Chui, M. L., Pu, Y., Gunda, S. T., Chen, Z., Qin, J., King, A. D., Chu, W. C. W., Cai, J., & Ying, M. T. C. (2025). The Application of Deep Learning for Lymph Node Segmentation: A Systematic Review. *IEEE Access*, *13*, 97208–97227. https://doi.org/10.1109/ACCESS.2025.3575454

[4] Wang, L. (2022). Deep Learning Techniques to Diagnose Lung Cancer. *Cancers*, *14*(22), 1–24. https://doi.org/10.3390/cancers14225569

[5] Amarasinghe, N. H., & Ambegoda, T. D. (2024). Few-Shot Lung Cancer Classification Using Prototypical Networks. *ICARC 2024 - 4th International Conference on Advanced Research in Computing: Smart and Innovative Trends in Next Generation Computing Technologies*, 79–84. https://doi.org/10.1109/ICARC61713.2024.10499732

[6] Hallitschke, V. J., Schlumberger, T., Kataliakos, P., Marinov, Z., Kim, M., Heiliger, L., Seibold, C., Kleesiek, J., & Stiefelhagen, R. (2023). Multimodal Interactive Lung Lesion Segmentation: A Framework for Annotating PET/CT Images Based on Physiological and Anatomical Cues. *Proceedings - International Symposium on Biomedical Imaging*, 1–5. https://doi.org/10.1109/ISBI53787.2023.10230334

[7] Kim, S., Lim, J. H., Kim, C. H., Roh, J., You, S., Choi, J. S., Lim, J. H., Kim, L., Chang, J. W., Park, D., Lee, M. won, Kim, S., & Heo, J. (2024). Deep learning–radiomics integrated noninvasive detection of epidermal growth factor receptor mutations in non-small cell lung cancer patients. *Scientific Reports*, *14*(1), 1–8. https://doi.org/10.1038/s41598-024-51630-6

[8] Shariff, V., Paritala, C., & Ankala, K. M. (2025). Optimizing non small cell lung cancer detection with convolutional neural networks and differential augmentation. *Scientific Reports*, *15*(1), 1–27. https://doi.org/10.1038/s41598-025-98731-4

[9] Du, D., Shiri, I., Yousefirizi, F., Salmanpour, M. R., Lv, J., Wu, H., Zhu, W., Zaidi, H., Lu, L., & Rahmim, A. (2025). Impact of harmonization and oversampling methods on radiomics analysis of multi-center imbalanced datasets: application to PET-based prediction of lung cancer subtypes. *EJNMMI Physics*, *12*(1), 1–16. https://doi.org/10.1186/s40658-025-00750-7

[10] Yuan, L., An, L., Zhu, Y., Duan, C., Kong, W., Jiang, P., & Yu, Q. Q. (2024). Machine Learning in Diagnosis and Prognosis of Lung Cancer by PET-CT. *Cancer Management and Research*, *16*, 361–375. https://doi.org/10.2147/CMAR.S451871

[11] Zhang, X., Dong, X., Saripan, M. I. bin, Du, D., Wu, Y., Wang, Z., Cao, Z., Wen, D., Liu, Y., & Marhaban, M. H. (2023). Deep learning PET/CT-based radiomics integrates clinical data: A feasibility study to distinguish between tuberculosis nodules and lung cancer. *Thoracic Cancer*, *14*(19), 1802–1811. https://doi.org/10.1111/1759-7714.14924

[12] Pal, O. K., Roy, S., Modok, A. K., Teethi, T. I., & Sarker, S. K. (2024). ULung:A Novel Approach for Lung Image Segmentation. *6th International Conference on Computing and Informatics, ICCI 2024*, 522–527. https://doi.org/10.1109/ICCI61671.2024.10485043

Gayap, H. T., & Akhloufi, M. A. (2024). Deep Machine Learning for Medical Diagnosis, Application to Lung Cancer Detection: A Review. *BioMedInformatics*, *4*(1), 236–284. https://doi.org/10.3390/biomedinformatics4010015

[13] Gouveia, M., Mendes, T., Rodrigues, E. M., Oliveira, H. P., & Pereira, T. (2025). Comparing 2D and 3D Feature Extraction Methods for Lung Adenocarcinoma Prediction Using CT Scans: A Cross-Cohort Study. *Applied Sciences (Switzerland)*, *15*(3), 1–22. https://doi.org/10.3390/app15031148

[14] Wehbe, A., Dellepiane, S., & Minetti, I. (2024). Enhanced Lung Cancer Detection and TNM Staging Using YOLOv8 and TNMClassifier: An Integrated Deep Learning Approach for CT Imaging. IEEE Access, 12, 141414–141424. https://doi.org/10.1109/ACCESS.2024.3462629

[15] Barbouchi, K., El Hamdi, D., Elouedi, I., Aïcha, T. Ben, Echi, A. K., & Slim, I. (2023). A transformer-based deep neural network for detection and classification of lung cancer via PET/CT images. International Journal of Imaging Systems and Technology, 33(4), 1–14. https://doi.org/10.1002/ima.22858

[16] Lin, J., Yu, Y., Zhang, X., Wang, Z., & Li, S. (2023). Classification of Histological Types and Stages in Non-small Cell Lung Cancer Using Radiomic Features Based on CT Images. Journal of Digital Imaging, 36(3), 1029–1037. https://doi.org/10.1007/s10278-023-00792-2

[17] Aksu, F., Gelardi, F., Chiti, A., & Soda, P. (2025). Multi-stage intermediate fusion for multimodal learning to classify non-small cell lung cancer subtypes from CT and PET. Pattern Recognition Letters,

193, 86–93. https://doi.org/10.1016/j.patrec.2025.04.001

[18] Bouamrane, A., Derdour, M., Bennour, A., Elfadil Eisa, T. A., M. Emara, A. H., Al-Sarem, M., & Kurdi, N. A. (2025). Toward Robust Lung Cancer Diagnosis: Integrating Multiple CT Datasets, Curriculum Learning, and Explainable AI. Diagnostics, 15(1), 1–18. https://doi.org/10.3390/diagnostics15010001

[19] Weikert, T., Jaeger, P. F., Yang, S., Baumgartner, M., Breit, H. C., Winkel, D. J., Sommer, G., Stieltjes, B., Thaiss, W., Bremerich, J., Maier-Hein, K. H., & Sauter, A. W. (2023). Automated lung cancer assessment on 18F-PET/CT using Retina U-Net and anatomical region segmentation. European Radiology, 33(6), 4270–4279. https://doi.org/10.1007/s00330-022-09332-y

[20] Ji, Z., Zhao, J., Liu, J., Zeng, X., Zhang, H., Zhang, X., & Ganchev, I. (2023). ELCT-YOLO: An Efficient One-Stage Model for Automatic Lung Tumor Detection Based on CT Images. Mathematics, 11(10), 1–22. https://doi.org/10.3390/math11102344

[21] Pal, S., & Mitra, S. (2025). Deep Ensembling with Multimodal Image Fusion for Efficient Classification of Lung Cancer. ArXiv, 1–7. https://arxiv.org/pdf/2502.00078